Monotonicity-preserving Interproximation of B-H-Curves*

Clemens Pechstein[1] and Bert Jüttler[2]

Special Research Program "Numerical and Symbolic Scientific Computing", Institute of Computational Mathematics and Institute of Applied Geometry, Johannes Kepler University Linz, Austria

Abstract

B-H-curves are used for modeling ferromagnetic materials in connection with electromagnetic field computations. Starting from real-life measurement data, we present an approximation technique which is based on the use of spline functions and a data-dependent smoothing functional. It preserves physical properties, such as monotonicity, and is robust with respect to noise in the measurements.

Key words: monotonicity-preserving approximation, interproximation, smoothing splines, B-H-curves, Maxwell's equations, nonlinear field computations

1 Introduction

B-H-curves, which describe the nonlinear relation between the magnetic induction (or flux density) $\boldsymbol{B}$ and the magnetic field $\boldsymbol{H}$, are needed for the modeling of ferromagnetic materials in connection with electromagnetic field computations. Due to the underlying physics, such curves are naturally monotone and must often be approximated from real-life measurements.

Based on different approaches (such as classical cubic splines, splines with free knots, exponential or rational splines), various methods for monotonicity-preserving interpolation of measurement data have been described in the literature (Fritsch and Carlson, 1980; Kopotun and Shadrin, 2003; Manni and Sablonnière, 1997; Oja, 1997; Pinchukov, 2001; Qu and Sarfraz, 1997; Volkov,

[1] Address: Altenberger Str. 69, 4040 Linz, Austria; E-Mail: `clemens.pechstein@numa.uni-linz.ac.at`
[2] Address: Altenberger Str. 69, 4040 Linz, Austria; E-Mail: `bert.juettler@jku.at`
* supported by the Austrian Science Foundation FWF under grant SFB F013

2001; Zavyalov and Bogdanov, 1995). A very general and powerful framework for shape-preserving interpolation and approximation has been developed by Dierckx (1993).

In the specific situation of B-H-curves, a method for monotonicity-preserving interpolation, which is based on earlier work using cubic splines (Fritsch and Carlson, 1980), has been described by Heise (1994). However, as a severe limitation, such interpolation techniques may have problems with noisy data. More recently, Reitzinger, Kaltenbacher and Kaltenbacher (2002) have proposed to approximate B-H-data by a so-called smoothing spline (see also Reinsch (1967)), balancing the deviation from the data vs. the L_2-norm of the second derivative. The balancing factor is obtained by an iterative procedure, according to the discrepancy principle, until monotonicity is achieved. Additionally, an extrapolation model for $H \to \infty$ is introduced.

Two key problems of this approach are the following. First, the uniqueness of the solution to the corresponding optimization problem is achieved only by imposing boundary conditions on the first derivatives at the two end points. However, the values of these boundary constraints (e. g., the first difference quotient of the boundary data) have a non-negligible influence on the shape of the curve. Consequently, the method looses flexibility. Second, the monotonicity is not a-priori guaranteed. According to numerical experiments with various real-life data sets, some sets of specific data could not be handled satisfactorily, and even monotonicity could not always be achieved. We believe that this was mainly caused by the influence of the boundary conditions.

In this paper, we extend the work in the following directions. In order to deal with the uncertainties (measurement errors) which are present in the data, we propose a method for *interproximation* (cf. Cheng and Barsky, 1991), where the resulting spline function always satisfies the monotonicity constraints. In addition, no boundary conditions have to be imposed. Instead, we propose to use a *data-dependent smoothing functional* in order to achieve a unique solution with good physical properties. As demonstrated by curves obtained from real-life data, using this functional we obtain curves which are both physically plausible and visually pleasing. Finally, the extrapolation for $H \to \infty$ is included in the spline interproximation by introducing a nonlinear transformation. This leads to a robust method which is able to handle rather uncertain data.

The remainder of the paper is organized as follows. In the next section we describe the problem and its physical background. Section 3 is devoted to the numerical realization using spline functions. Finally, we illustrate the results by several examples.

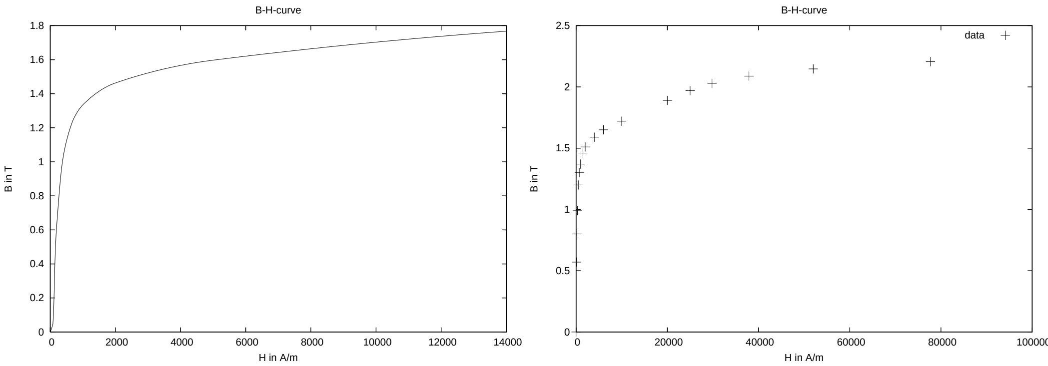

Fig. 1. Left: B-H-curve associated with a ferromagnetic material. Right: Measurements corresponding to another material.

2 Preliminaries

After a brief introduction to the properties of B-H-curves, we describe the approximation problem in some detail.

2.1 B-H-curves

A key feature in magnetic field computations is the nonlinear relation between the *magnetic induction (magnetic flux density)* $\boldsymbol{B}$ and the *magnetic field* $\boldsymbol{H}$. Considering the isotropic case and neglecting the effects of hysteresis, it is known that

$$\boldsymbol{B} = \mu(|\boldsymbol{H}|)\boldsymbol{H} \tag{1}$$

holds within a homogeneous material, where the function $\mu : \mathbb{R}_0^+ \to \mathbb{R}^+$ is called the *permeability* (cf. Ida and Bastos, 1997; Jackson, 1998). Consequently, the (three-dimensional) vector fields $\boldsymbol{B}$ and $\boldsymbol{H}$ are always parallel.

Introducing $f(s) := \mu(s)s$, we have

$$|\boldsymbol{B}| = f(|\boldsymbol{H}|), \tag{2}$$

where the function $f : \mathbb{R}_0^+ \to \mathbb{R}_0^+$ is usually called *B-H-curve* (cf. Fig. 1, left). In practice, such material curves are never given in an analytic form. Instead, they have to be approximated from measurements (Fig. 1, right).

Since in the magnetostatic case, $\boldsymbol{H}$ and $\boldsymbol{B}$ depend only on the *current density* $\boldsymbol{J}$, one usually chooses various densities $(\boldsymbol{J}_k)_{k=1}^N$ and performs measurements in the corresponding material. Eventually, this leads to finitely many pairs

$$(H_k, B_k), \quad k = 1, \ldots, N, \tag{3}$$

with $H_k = |\boldsymbol{H}(\boldsymbol{J}_k)|$, $B_k = |\boldsymbol{B}(\boldsymbol{J}_k)|$, which are affected by noise (measurement errors), i. e.

$$\Big|f(H_k) - B_k\Big| \leq \delta_k, \quad \text{for } k = 1, \ldots, N. \tag{4}$$

If no information about the accuracy of the measurements is available, one may assume that $\delta_k = 0.01 \cdot |B_k|$.

In addition to these measurements, we set $B_0 = H_0 = 0$.

Since any nonlinear magnetic field problem and its solution heavily depend on the underlying B-H-curves, the approximation of those must preserve all their physical properties, which are formulated in the following assumptions:

(A1) f is continuously differentiable on $\mathbb{R}_0^+$,
(A2) $f(0) = 0$,
(A3) $f'(s) \geq \mu_0, \quad \forall s \geq 0$,
(A4) $\lim_{s\to\infty} f'(s) = \mu_0$,

where the constant $\mu_0 = 4\,\pi \cdot 10^{-7}$ denotes the permeability in vacuum. From (A1)–(A4), one can deduce further properties which are essential for the analysis of magnetic field problems and for computations:

1. f is strongly monotone with monotonicity constant μ_0:

$$\Big(f(s) - f(t)\Big)(s - t) \geq \mu_0 |s - t|^2, \quad \forall s, t \geq 0.$$

2. f' is continuous and bounded:

$$\mu_0 \leq f'(s) \leq L := \sup_{t\geq 0} f'(t) < \infty, \quad \forall s \geq 0.$$

   Consequently, f is (globally) Lipschitz-continuous with Lipschitz constant L.
3. f is bijective on $\mathbb{R}_0^+$ and therefore has an inverse f^{-1}.
4. f^{-1} is continuously differentiable with

$$m := \frac{1}{L} \leq \left(f^{-1}\right)'(s) \leq \nu_0 := \frac{1}{\mu_0}, \quad \forall s \geq 0.$$

5. The so-called *reluctivity* function $\nu(s) := f^{-1}(s)/s$ is well-defined for $s \geq 0$, and furthermore continuous and bounded with

$$\begin{aligned} m \leq \nu(s) &\leq \nu_0, \qquad \forall s \geq 0, \\ \lim_{s\to 0} \nu(s) &= \left(f^{-1}\right)'(0), \\ \lim_{s\to\infty} \nu(s) &= \nu_0. \end{aligned}$$

6. $\nu(s)s = f^{-1}(s)$ is strongly monotone with monotonicity constant m and Lipschitz-continuous with Lipschitz constant ν_0.

7. ν is continuously differentiable on $(0, \infty)$ and

$$\lim_{s \to \infty} \nu'(s) = 0.$$

If ν is differentiable in 0 and f twice differentiable in 0, then

$$\nu'(0) = \frac{1}{2}(f^{-1})''(0).$$

For a detailed verification of these properties see Pechstein (2004).

Due to the relation

$$\boldsymbol{H} = \nu(|\boldsymbol{B}|)\boldsymbol{B}, \tag{5}$$

the reluctivity function ν and also its derivative ν' are needed in computations corresponding to nonlinear eddy current and magnetostatic problems. Note that the strong monotonicity of $\nu(s)s$ implies the solvability of the nonlinear magnetostatic problem and guarantees the convergence of Newton's method whenever ν' exists. See Heise (1991, 1994); Pechstein (2004) for additional information.

2.2 The approximation problem

The B-H-curve f has to be approximated by some function $\tilde{f}$ satisfying both (A1)–(A4) for $\tilde{f}$ and

$$|\tilde{f}(H_k) - B_k| \leq c\,\delta_k, \quad \text{for } k = 1, \ldots, N, \tag{6}$$

for some constant $c > 0$, i. e. the approximation error should remain in the range of the measuring error (cf. Reitzinger, Kaltenbacher and Kaltenbacher (2002); Dierckx (1993)). The strong monotonicity (A3) is essential, since it guarantees that f is bijective, and – as a consequence thereof – that the reluctivity function ν is well-defined.

For the numerical simulation of nonlinear magnetic field problems, one needs very fast procedures for evaluating the functions ν and ν', also for values $B > B_N$. That is, the B-H-curve must be approximated on the domain set $\mathbb{R}_0^+$ (cf. (A4)).

The original B-H-curve has infinite domain and infinite range. We now reduce the approximation problem to the approximation with a monotone function with finite both domain and range.

First, we set

$$\tilde{f}(s) := g(s) + \mu_0\, s, \tag{7}$$

with

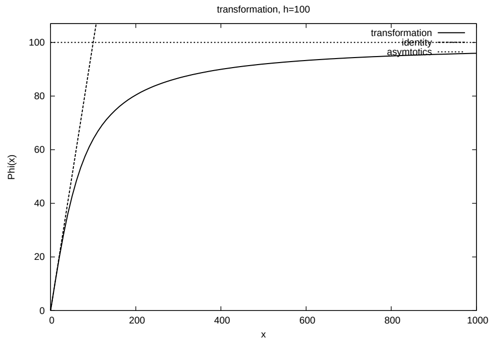

Fig. 2. The transformation $\Phi(x) = \frac{2}{\pi}\, h_\infty \arctan\left(\frac{\pi}{2}\,\frac{x}{h_\infty}\right)$ with $h_\infty = 100$.

- $g : \mathbb{R}_0^+ \to [0, g_{\max}]$ continuously differentiable,
- $g(0) = 0$,
- $g'(s) \geq 0, \quad \forall s \geq 0$,
- $\lim_{s\to\infty} g'(s) = 0$.

Second, choosing certain suitable values $H_* \geq H_N$ and $h_\infty > 0$, we represent the function g on $[H_*, \infty)$ by some function $\hat{g}$ on $[H_*, H_\infty)$, with $H_\infty := H_* + h_\infty$:

$$g(s) = \begin{cases} \hat{g}\Big(H_* + \Phi(s - H_*)\Big) & \text{for } s \geq H_*, \\ \hat{g}(s) & \text{elsewhere,} \end{cases} \tag{8}$$

with a $\mathcal{C}^\infty$ bijective transformation $\Phi : \mathbb{R}_0^+ \to [0, h_\infty)$ which is both strongly monotone and fulfills $\Phi'(0) = 1, \Phi''(0) = 0$. A possible choice for this bijective transformation is

$$\Phi(x) := \frac{2}{\pi}\, h_\infty \arctan\left(\frac{\pi}{2}\,\frac{x}{h_\infty}\right).[2] \tag{9}$$

This setup ensures that g is $\mathcal{C}^2$ on $[H_*, H_\infty)$ if and only if $\hat{g}$ is $\mathcal{C}^2$. Additionally,

$$g'(s) \geq 0 \quad \Longleftrightarrow \quad \hat{g}'(s) \geq 0, \tag{10}$$

owing to $\Phi'(s) > 0$; and $\lim_{s\to\infty} g'(s) = 0$ since $\lim_{s\to\infty} \Phi'(s) = 0$. Note that the choice of h_∞ and the value of $\hat{g}(H_\infty)$ determine how fast $\lim_{s\to\infty} \tilde{f}(s) = \mu_0$ converges.

2.3 Interproximation and smoothing conditions

We assume that a sequence of data

$$(H_k, \hat{B}_k + \mu_0\, H_k), \quad k = 0, \ldots, N, \tag{11}$$

[2] Another one is $\Phi(x) = h_\infty\big[1 - e^{-1/2\,(x/h_\infty)^2 - x/h_\infty}\big]$.

is given, where

$$
\begin{aligned}
0 = H_0 < H_1 < \cdots < H_N \le H_*, \\
0 = \hat{B}_0 \le \hat{B}_1 \le \cdots \le \hat{B}_N < \infty.
\end{aligned}
\tag{12}
$$

The function $\hat{g}$ has to fulfill the conditions

(B1) $\hat{g} \in \mathcal{C}^1([0, H_\infty] \to \mathbb{R}_0^+)$,
(B2) $\hat{g}'(s) \ge 0, \quad \forall s \ge 0$,
(B3) $\hat{g}(0) = 0$ (and optionally $\hat{g}'(H_\infty) = 0$),
(B4) $|\hat{g}(H_k) - \hat{B}_k| \le c\,\delta_k, \quad$ for $k = 1, \ldots, N$.

In order to find a good approximation, we minimize some functional $F[g]$, measuring the smoothness of the result, in some spline space $\mathcal{V}$, subject to (B1)–(B4). A first suggestion is the L_2-norm of the second derivative (or linearized strain energy) [3]

$$
F[g] := \int_0^{H_\infty} [\hat{g}''(s)]^2 \, \mathrm{d}s \quad \longrightarrow \quad \min_{\hat{g} \in \mathcal{V}} . \tag{13}
$$

It is well-known that an *interpolating* cubic $\mathcal{C}^2$-spline with its knots at H_k minimizes this energy.

As to be demonstrated by the examples (e. g. the data set `QMS3L`, see Fig. 5 on page 13), this simple functional often produces unsatisfactory results. This is due to a characteristic feature of B-H-curves that the first derivative varies enormously, from "very steep" to "very flat".

In order to address these problems, we propose to use another, data-dependent functional. First, $\hat{g}$ is individually scaled on each interval $[H_k, H_{k+1}]$ such that it maps $[0, 1]$ to $[0, 1]$:

$$
\hat{g}_{\text{scaled}}(s) := \frac{\hat{g}\Big(H_k + s\,(H_{k+1} - H_k)\Big) - \hat{B}_k}{\hat{B}_{k+1} - \hat{B}_k}.
$$

We arrive at the following identity for the scaled linearized strain energy:

$$
\int_0^1 \left[\frac{\mathrm{d}^2}{\mathrm{d}s^2} \hat{g}_{\text{scaled}}(s)\right]^2 \mathrm{d}s = \int_{H_k}^{H_{k+1}} \left[\frac{\mathrm{d}^2}{\mathrm{d}x^2} \hat{g}(x)\right]^2 \frac{(H_{k+1} - H_k)^3}{(\hat{B}_{k+1} - \hat{B}_k)^2} \, \mathrm{d}x.
$$

In order to avoid possible numerical problems for small differences $\hat{B}_{k+1} - \hat{B}_k$, [4] we regularize with some ε-term, where $0 < \varepsilon \ll 1$ (e. g., $\varepsilon = 10^{-7}$).

---

[3] Another possible objective function is $F[g] := \int_0^\infty [g''(s)]^2 \, \mathrm{d}s$, involving the transformation Φ.
[4] Note, that these differences are only guaranteed to be nonnegative.

Summing up, the functional reads

$$F_{\text{scaled}}[g] = \int_0^{H_\infty} [\hat{g}''(s)]^2 \frac{\mathrm{d}s}{\omega(s)} \quad \to \quad \min_{\hat{g}\in\mathcal{V}}, \tag{14}$$

with the piecewise constant weight

$$\begin{aligned} \omega(s) &= \frac{1}{H_{k+1}-H_k}\left[\left(\frac{\hat{B}_{k+1}-\hat{B}_k}{H_{k+1}-H_k}\right)^2 + \varepsilon\left(\frac{\hat{B}_N}{H_N}\right)^2\right], \quad \text{for } s\in[H_k,H_{k+1}), \\ \omega(s) &= \frac{1}{H_N-H_{N-1}}\left[\left(\frac{\hat{B}_N-\hat{B}_{N-1}}{H_N-H_{N-1}}\right)^2 + \varepsilon\left(\frac{\hat{B}_N}{H_N}\right)^2\right], \quad \text{for } s\geq H_N, \end{aligned} \tag{15}$$

As an essential property of any smoothing functional in this application, the result should not depend on the scaling of the two coordinate axes. It can easily be verified that this is true both for the original functional $F[g]$ and for the modified one $F_{\text{scaled}}[g]$. However, it would not be satisfied for the real nonlinear bending energy $\int \kappa^2\sqrt{1+f'^2}\,\mathrm{d}s$, where κ is the curvature of the graph $(s, f(s))$. Consequently, the use of this energy is not appropriate for this application!

The results obtained by using the two different functionals will be compared in Section 4.

3 Numerical realization

We recall the definition of B-splines and adapt the description of spline functions to our specific application. This reduces the problem to a quadratic programming problem.

3.1 B-splines

For any degree d, consider some knots $(\lambda_i)_{i=0}^n$ with

$$0 = \lambda_0 \leq \lambda_1 \leq \cdots \leq \lambda_n = H_\infty, \tag{16}$$

satisfying $\lambda_i < \lambda_{i+d+1}$. In addition, the boundary knots are assumed to have multiplicity $d+1$, $\lambda_0 = \lambda_d$ and $\lambda_{n-d} = \lambda_n$.

Any piecewise polynomial function of degree d on the partition defined by these knots which is $\mathcal{C}^{d-m}$ at the knot λ_j, where this knot has multiplicity [5]

[5] I. e., the m neighboring knots are identical.

m, can be written in the B-spline representation

$$\hat{g}(s) = \sum_{i=0}^{n-d-1} x_i \, N_{i,d+1}(s), \quad s \in [\lambda_0, \lambda_n], \tag{17}$$

where $N_{i,d+1}$ denotes the i-th normalized B-spline of degree d with respect to the knots $(\lambda_i)_{i=0}^{n}$ (cf. Dierckx, 1993).

In our applications, we assume that every inner knot appears with the fixed multiplicity l (i. e. the spline function is in $\mathcal{C}^{d-l}$), and consider the following variants:

(V.1) Quadratic $\mathcal{C}^1$ splines, $d = 2$, $l = 1$. The set of inner knots are the given values H_k with one additional knot per interval.

(V.2) Cubic $\mathcal{C}^1$ splines. The set of knots are again the given values H_k, but counted with multiplicity $l = 2$.

(V.3) Cubic $\mathcal{C}^2$ splines. Two knots $H_k - \Delta_k, H_k + \Delta_k$ are placed around each given value H_k with a small distance $2\Delta_k$ between them ("torn" version of V.2).

The spline space $\mathcal{V}$, the constraints and the objective function above could be described by the coefficients (x_i). However, in our case it is more appropriate to use a slightly different approach. It is known that the first derivative can be representated with lower degree basis functions, to wit

$$\hat{g}'(s) = \sum_{j=1}^{n-d-1} \bar{x}_j \, N_{j,d}(s). \tag{18}$$

Due to (B3), i. e. $\hat{g}(0) = 0$, the coefficients $(\bar{x}_j)$ determine the entire spline function $\hat{g}$. Hence,

$$\hat{g}(s) = \sum_{j=1}^{n-d-1} \bar{x}_j \, b_j(s), \tag{19}$$

where the basis functions b_j can be computed from the knots and from the parameters d and l. The following formulas give a one-to-one correspondence between the coefficients x_i and $\bar{x}_i$ (see also Dierckx, 1993):

$$\begin{aligned} &\bar{x}_i = (x_i - x_{i-1}) \frac{d}{\lambda_{i+d} - \lambda_i}, \qquad \forall i = 1, \ldots, n-d-1, \\ &x_0 = 0, \quad x_i = x_{i-1} + \frac{\lambda_{i+d} - \lambda_i}{d} \bar{x}_i, \qquad \forall i = 1, \ldots, n-d-1. \end{aligned} \tag{20}$$

Since the basis functions $N_{j,d}$ are non-negative, we conclude that

$$\bar{x}_j \geq 0, \quad \forall j = 1, \ldots, n-d-1 \quad \Longrightarrow \quad \hat{g}'(s) \geq 0, \quad \forall s \geq 0. \tag{21}$$

The other direction holds only if $d \leq 2$. However, for $d = 3$ this stronger version of assumption (B2) leads to satisfactory results too.[6]

3.2 Formulation as a quadratic programming problem

Introducing the matrices

$$(G)_{ij} := \int_0^{H_\infty} b_i''(t)\, b_j''(t)\, \frac{\mathrm{d}t}{\omega(t)}, \quad i, j = 1, \ldots, n-d-1, \tag{22}$$

$$(A)_{kj} := b_j(H_k), \quad k = 1, \ldots, N, \quad j = 1, \ldots, n-d-1, \tag{23}$$

we arrive at the optimization problem

$$\frac{1}{2}\, \bar{x}^T\, G\, \bar{x} \quad \rightarrow \quad \min_{\bar{x}} \tag{24}$$

subject to

$$\vec{B} - c\,\vec{\delta} \leq A\,\bar{x} \leq \vec{B} + c\,\vec{\delta}, \tag{25}$$

$$0 \leq \bar{x}, \tag{26}$$

where $\bar{x} = (\bar{x}_j)_{j=0}^{n-d-1}$, $\vec{B} = (\hat{B}_k)_{k=1}^{N}$, $\vec{\delta} = (\delta_k)_{k=1}^{N}$, and the inequalities are understood component-wise. Setting $\bar{x}_{n-d-1} = 0$ corresponds to the right boundary condition in (B3) and can easily be incorporated into the system.

The problem (24)–(26) is a standard quadratic programming problem with the positive semidefinite matrix G in the quadratic part of the objective and with linear box constraints. Such problems can be solved with the active set method or inner point methods (cf. Gill, Murray and Wright, 1981; Dierckx, 1993).

3.3 Existence of solutions

We assume now that the data is well-posed, i. e. (12), and consider only the variants V.1 and V.2.

First, we see that the matrix G is always positive semidefinite, because $\bar{x}^T G \bar{x} \geq 0$ due to the definition of $F[g]$ or $F_{\mathrm{scaled}}[g]$. Secondly, the linear box constraints result in a convex feasibility polyhedron. Since one can easily construct a monotone *interpolating* spline with vanishing first derivative in the

[6] Generally, this construction leads to linear sufficient conditions for monotonicity. Weaker conditions can easily be generated by inserting additional "phantom knots", which do not contribute any new degrees of freedom, but which are used only for generating the B-spline representation. See Jüttler (1997) for more information on this technique.

data points, this feasibility domain is nonempty. Hence, at least one solution of the quadratic programming problem exists.

The solution is not necessarily unique, since the functional may be constant on one of the boundary polytopes of the feasible domain. In order to achieve uniqueness, the functional can be regularized by

$$F_{\mathrm{reg}}[g] := F_{(\mathrm{scaled})}[g] + \varepsilon_1 \sum_{i=1}^{N} \left(\hat{g}(H_i) - \hat{B}_i\right)^2 + \varepsilon_2 \sum_{k=1}^{n} \left(\hat{g}''(\lambda_k^+) - \hat{g}''(\lambda_k^-)\right)^2, \quad (27)$$

with the two regularization parameters ε_1, ε_2. However, according to our numerical experiments, this issue is only of theoretical importance.

4 Numerical results and concluding remarks

We illustrate the method by several numerical examples. Next we discuss efficient methods for evaluating B-H-curves and their inverses, which are needed for FEM computations. Finally, we conclude this paper.

4.1 Examples

All the following results (Figures 3, 4, 5, 6) were obtained with the parameters

$$\begin{aligned} H_* &= H_N, & h_\infty &= \max\{H_N/3, H_N - H_{N-1}\}, \\ \delta_k &= 0.005 \cdot B_k, \ \text{and} & c &= 1. \end{aligned}$$

The optimization problem was solved using a code by Helmut Gfrerer (Linz), which is based on a variant of the active set method.

In the first example, we applied the method to the data set `Su7a2` (all data are Courtesy of Robert Bosch GmbH). We show the interproximating B-H-curve f which was obtained using V.2, its first and second derivatives, and the associated reluctivity function. This curve is to be compared with the result obtained by using V.3 (third row), where the second derivative is still continuous (right).

The second example (data set `SiF2`) shows the advantages of using interproximation instead of interpolation. Due to the tolerance, the last two (uncertain) measuring points (marked by crosses) do not affect the natural shape of the B-H-curve too much, see Fig. 4, left.

In order to visualize the self-similarity of the curve, we have plotted the curve for smaller values of H.

The third example (data set `QMS3L`) demonstrates the influence of the two different smoothing terms. The left curve in Fig. 5 has been generated using

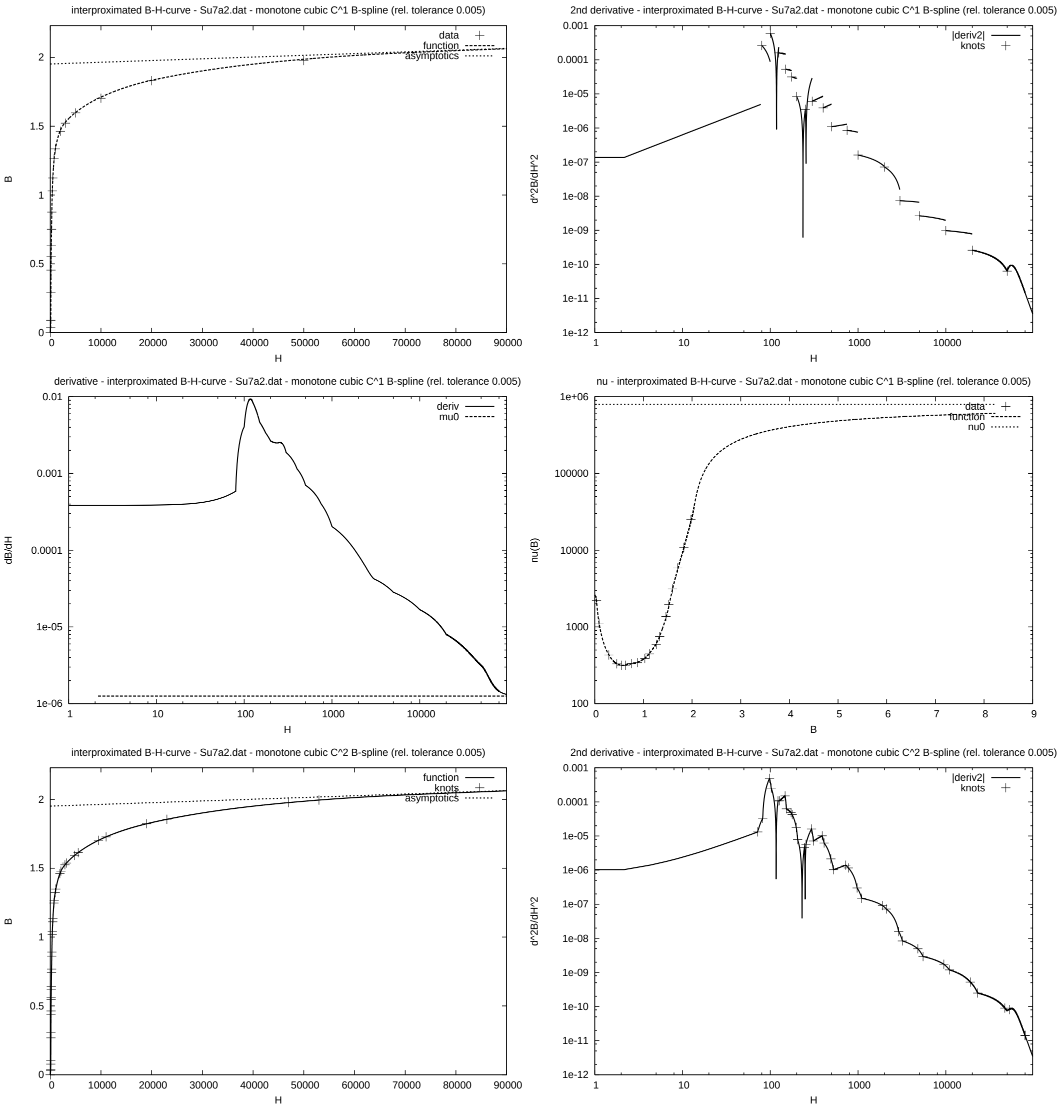

Fig. 3. Results for data set `Su7a2`. Upper left: approximated B-H-curve using V.2; upper right: its second derivative; middle left: its first derivative; middle right: the reluctivity function ν; lower left: approximation using V.3 (torn knots, $\mathcal{C}^2$-spline); lower right: corresponding (continuous) second derivative.

the classical linearized strain energy $F[g]$, while the right curve minimizes the data-dependent functional $F_{\text{scaled}}[g]$. The right curve is more physically plausible and visually pleasing than the other result.

Finally, we compare the results obtained by using V.1 and V.2, see Fig. 6.

According to our experience, cubic $\mathcal{C}^1$-splines $(d = 3, l = 2)$ gave the best results for the problem of monotonicity-preserving B-H-curve interproximation. This is probably due to the well-known fact that any monotone data can be interpolated with a monotone cubic $\mathcal{C}^1$-spline but in general not with a monotone $\mathcal{C}^2$-spline (cf. Fritsch and Carlson, 1980; Reitzinger, Kaltenbacher and Kaltenbacher, 2002).

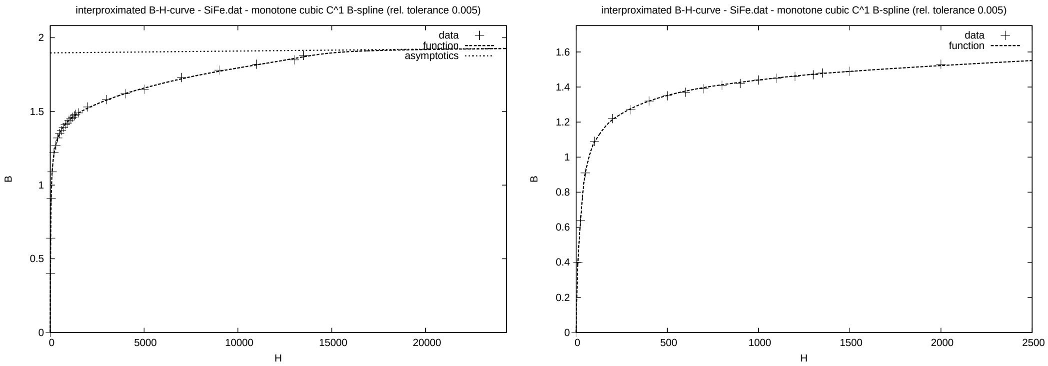

Fig. 4. V.2 applied to the data set `SiF2`.

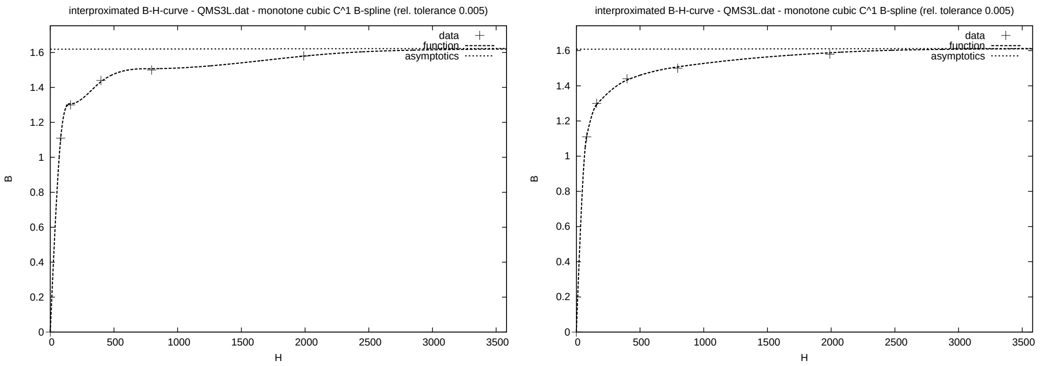

Fig. 5. V.2 applied to the data set `QMS3L`. Left: Minimization of $F[g]$: $F[g] = 2.267 \cdot 10^{-6}$, $F_{\text{scaled}} = 16.944$. Right: Minimization of $F_{\text{scaled}}[g]$: $F[g] = 4.069 \cdot 10^{-6}$, $F_{\text{scaled}} = 3.476$.

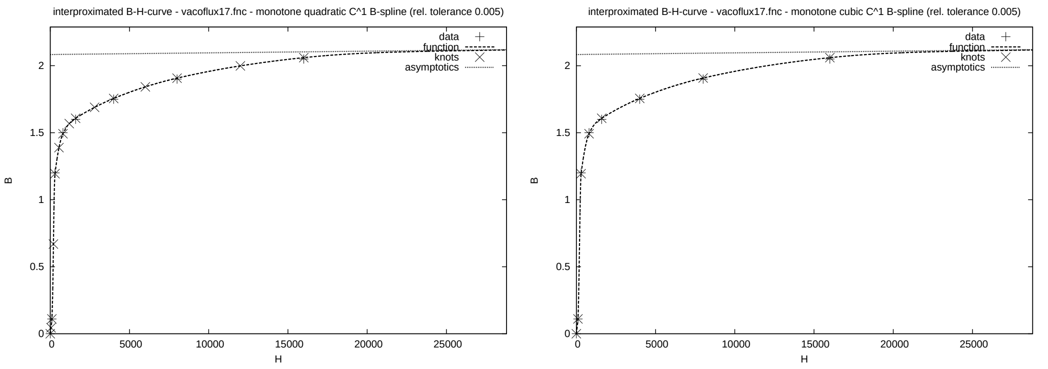

Fig. 6. Results for data set `vacoflux17`. Left: V.1 – Quadratic $\mathcal{C}^1$-spline with additional knots. Right: V.2 – Cubic $\mathcal{C}^1$-spline.

4.2 Evaluating the B-H-curve and its inverse

During nonlinear magnetic field computations via FEM, one needs a high number of evaluations of μ and μ', for the scalar potential formulation, or ν and ν', for the vector potential formulation (cf. Heise, 1994; Pechstein, 2004; Ida and Bastos, 1997). Here, the direct evaluation of f and of its derivative by using either the definition of the B-spline or de Boor's algorithm is too expensive. Instead, we recommend to calculate – for each segment of the spline function – the polynomial representation of the spline function, as a postprocessing step after the optimization. This polynomial can then efficiently be evaluated, e. g., with Horner's method.

The inverse function f^{-1} (which is needed in order to evaluate ν, ν') can efficiently be computed using Newton's method together with a lookup table of initial values to keep the number of iterations small (see Reitzinger, Kaltenbacher and Kaltenbacher, 2002). Here, the use of a $\mathcal{C}^2$ solution may result in better convergence, although the practical benefits seem to be rather small. On the other hand, by using quadratic splines (V.1), the inverse function can be expressed explicitly by solving a single quadratic equation.

4.3 Conclusion

We presented a method for monotonicity-preserving interproximation of measurement data, which has been adapted to the special case of B-H-curves. As shown by the examples, the use of data-dependent functionals, and interproximation instead of interpolation, helps to obtain physically plausible and visually pleasing results.

In principle, the approximation algorithm presented in this paper can be extended to the interproximation of any monotone functions (with or without certain constraints). For instance, characteristic curves in plasticity can be generated using a similar approach.

Efficient methods for evaluating the resulting spline curves are important for FEM computations. Here, the use of quadratic spline curves may be an advantage, since an explicit representation of the inverse function is available.

Acknowledgments. We thank Robert Bosch GmbH (Dept. FV/FLO3 at Gerlingen, Germany), in particular Volker Rischmüller, for providing the real-life data sets. Furthermore, we are indebted to Helmut Gfrerer (Linz) for advise and fruitful discussions concerning optimization. The financial support of this research by the Austrian Science Fund (FWF) is gratefully acknowledged. Last, but not least, we are grateful to Ulrich Langer (Linz) for his encouragement and support of this work.

References

F. Cheng, B. A. Barsky (1991): Interproximation: Interpolation and Approximation using Cubic Spline Curves, Computer-Aided Design **23**, 700–706.

P. Dierckx (1993): *Curve and Surface Fitting with Splines*, Oxford Science Publications.

S. Fredenhagen, H. J. Oberle, G. Opfer (1999): On the construction of optimal monotone cubic spline interpolations, J. Approximation Theory **96**, 182–201.

F. N. Fritsch, R. E. Carlson (1980): Monotone Piecewise Cubic Interpolation, SIAM J. Numer. Anal. **2**, 235–246.

P. E. Gill, W. Murray, M. H. Wright (1981): *Practical Optimization*, Academic Press, London and New York.

G. Greiner, A. Kolb and A. Riepl (2002): Scattered Data Interpolation Using Data Dependant Optimization Techniques, Graph. Models **64**, No. 1, 1–18.

B. Heise (1994): Analysis of a fully discrete Finite Element Method for a Nonlinear Magnetic Field Problem, SIAM J. Numer. Anal. **31**, 745–759.

B. Heise (1991): *Mehrgitter-Newton-Verfahren zur Berechnung nichtlinearer magnetischer Felder*, PhD-Thesis, Technical University of Chemnitz (Germany).

N. Ida, J. P. A. Bastos (1997): *Electromagnetics and Calculation of Fields*, Springer.

J. D. Jackson (1998): *Classical Electrodynamics*, Wiley, New York, third edition.

B. Jüttler (1997): Surface fitting using convex tensor–product splines, Journal of Computational and Applied Mathematics **84**, 23–44.

K. Kopotun, A. Shadrin (2003): On k-monotone approximation by free knot splines. SIAM J. Math. Anal. **34**, 901–924.

C. Manni, P. Sablonnière (1997): Monotone interpolation of order 3 by C^2 cubic splines, IMA J. Numer. Anal. **17**, 305–320.

P. Oja (1997): Low degree rational spline interpolation, BIT **37**, 901–909.

C. Pechstein (2004): *Multigrid-Newton-Methods for Nonlinear Magnetostatic Problems*, Master Thesis, Johannes Kepler University Linz, Austria. Available from `www.numa.uni-linz.ac.at`.

V. I. Pinchukov (2001): A monotone nonlocal cubic spline, Comput. Math. Math. Phys. **41**, 180–186.

R. Qu, M. Sarfraz (1997): Efficient method for curve interpolation with monotonicity preservation and shape control, Neural Parallel Sci. Comput. **5**, 275–288.

C. H. Reinsch (1967): Smoothing by Spline Functions, Numer. Math. **10**, 177–183.

S. Reitzinger, B. Kaltenbacher, M. Kaltenbacher (2002). A Note on the Approximation of B-H Curves for Nonlinear Computations, Report no. 02-30, SFB F013, Johannes Kepler University Linz, Austria. Available from `www.sfb013.uni-linz.ac.at`.

Yu. S. Volkov (2001): On monotone interpolation by cubic splines, Vychisl. Tekhnol. **6**, 14–24.

Yu. S. Zavyalov, V.V. Bogdanov (1995): Monotone and convex Hermite interpolation by generalized cubic splines, Sib. J. Comput. Math. **2**, 15–32.